Pressure-induced insulator-metal transitions in solid xenon and hydrogen: A first-principles quasiparticle study

Hélio Chacham,* Xuejun Zhu, and Steven G. Louie
Department of Physics, University of California, Berkeley, California 94720
and Materials Science Division, Lawrence Berkeley Laboratory, Berkeley, California 94720
(Received 13 April 1992)

We report a quasiparticle study of the pressure-induced isostructural insulator-metal transition in solids by the mechanism of band-gap closure. Two examples are investigated: solid Xe and molecular solid hydrogen. The band gaps are calculated with a first-principles quasiparticle approach, in which the electron self-energy operator is expanded to first order in the screened Coulomb interaction, viz., the GW approximation. For the case of solid xenon, the crystal structure has been experimentally established to be hexagonal-close-packed (hcp) in the vicinity of the observed metallization pressure of 132($\pm$5) GPa. Our calculation for solid xenon yields a metallization pressure of 128 GPa, in good agreement with experiment. The theoretical results further quantitatively explain all the salient features observed in the experimental optical spectra at metallization. For molecular solid hydrogen the structure has yet to be determined definitively. Our calculations are carried out for structures in which hydrogen molecules assume an hcp arrangement. The quasiparticle results are compared with those from Hartree-Fock (HF) and local-density approximation (LDA) calculations. In addition to the well-known HF overestimate and the LDA underestimate of the band gap, we find that both HF and LDA predict a linear behavior in the band gap versus density, whereas the quasiparticle results do not show such a linearity. This difference results from a significant increase in the dielectric screening with density, which gives rise to a strong and nontrivial dependence of the self-energy correction to the LDA band gap on density. We have also studied the effects of orientational disorder of the H_2 molecules within a virtual-crystal model. We find that at a given density, the minimum band gap increases monotonically and nonlinearly with orientational disorder. A simple tight-binding picture provides a convenient way to understand the variation of the hydrogen band gap both with pressure and with disorder. Our calculations predict a metallization pressure of 151 GPa for the hcp phase if the molecules are perfectly aligned along the c axis, and 300 GPa if there is no orientational order. At present, a definitive conclusion is difficult to draw as regards the metallization of molecular solid hydrogen. More details of the crystal structure, especially those concerning the orientational ordering of molecular H_2 at megabar pressures, are needed.

I. INTRODUCTION

The notion that any insulating crystal will eventually become metallic at a high enough pressure is well known and was put forward in the early days of quantum theory.[1] The metallization is expected to occur through one of three processes.

(a) The material becomes metallic by a pressure-induced structural transformation. Silicon under pressure is a well-known example of this case.[2]

(b) The material, which is an antiferromagnetic insulator at low pressures, becomes metallic by a simultaneous magnetic and metal-insulator transition. Such is the case of NiI_2, for instance.[3]

(c) The material becomes metallic without any concomitant structural or magnetic phase transitions. This is the case of solid Xe.[4,5]

Among these three processes, (a) is not a true electronic transition in that the metal-insulator transformation is a byproduct of a structural modification. Both (b) and (c) are electronic in nature. A quantitative calculation for realistic materials of process (b), which involves strong electron-correlation effects in a Mott insulator, is difficult using present-day first-principles theoretical techniques. On the other hand, process (c) usually involves the overlap of the valence and the conduction quasiparticle bands in band insulators, and is amenable to study with existing techniques by calculating the variation of the band gap with pressure.

In the present work, we investigate the band-gap closure in solid xenon and hydrogen under megabar pressures.[6] We make use of a first-principles quasiparticle technique[7] that, unlike the Hartree-Fock (HF) or the local-density approximation (LDA), reproduces accurately the band gaps of insulators and semiconductors[7] and therefore can be applied to a quantitative investigation of metallization due to band-gap closure. In Sec. II we give a brief description of the theoretical techniques for calculating the quasiparticle energies and the optical properties. Section III contains our results for the metallization transition in solid xenon. In Sec. IV we present our results for molecular solid hydrogen, including studies of the orientational disorder effects and the optical properties. Finally, a summary is given in Sec. V.

II. THEORETICAL APPROACH

A. Quasiparticle energies

The transport and optical properties of a solid are governed by its quasiparticle spectrum and its collective excitations. In the theoretical approach[7] used in this work, the quasiparticle energies $E_{n\mathbf{k}}$ are determined from the Dyson equation:

$$(T+V_n+V_H)\psi_{n\mathbf{k}}(\mathbf{r})+\int d\mathbf{r}'\Sigma(\mathbf{r},\mathbf{r}';E_{n\mathbf{k}})\psi_{n\mathbf{k}}(\mathbf{r}') = E_{n\mathbf{k}}\psi_{n\mathbf{k}}(\mathbf{r}) , \quad (1)$$

where T is the kinetic-energy operator, V_n is the potential due to the nuclei, V_H is the Hartree potential, and Σ is the electron self-energy operator. The following approximations have been used in solving Eq. (1).

(i) The self-energy operator is taken to be the first term in an expansion in the dynamically screened Coulomb interaction:[7]

$$\Sigma_{\mathrm{GW}}=\frac{i}{2\pi}\int d\omega\, e^{-i\delta\omega}G(\mathbf{r},\mathbf{r}',E-\omega)W(\mathbf{r},\mathbf{r}',\omega) . \quad (2)$$

This is the so-called GW approximation, which has been shown to yield very accurate electronic excitation energies for insulators, semiconductors, and semiconductor surfaces.[7] In Eq. (2), $W=\epsilon^{-1}V_C$ is the screened Coulomb interaction. The electron Green's function G is given in the quasiparticle approximation by

$$G(\mathbf{r},\mathbf{r}',E-\omega)=\sum_i \frac{\psi_i^*(\mathbf{r})\psi_i(\mathbf{r}')}{(E-\omega)-E_i-i\delta_i} , \quad (3)$$

where $\delta_i=0^+$ for a quasihole and $\delta_i=0^-$ for a quasielectron.

(ii) The wave functions ψ_i in Eqs. (1) and (3) have been shown to be well approximated[7] by the solutions to the Kohn-Sham equations in the local-density approximation[8] (LDA):

$$(T+V_n+V_H+V_{\mathrm{xc}})\psi_{n\mathbf{k}}(\mathbf{r})=E_{n\mathbf{k}}\psi_{n\mathbf{k}}(\mathbf{r}) , \quad (4)$$

where V_{xc} is the exchange-correlation potential. We use the Ceperley-Alder form[9] of the V_{xc} throughout this paper. The energy spectrum and the character of the wave function in Eq. (3) which determine the signs of δ_i in Eq. (3) must be consistent with the final quasiparticle band structure. This is important in our calculations, since the LDA band overlap occurs at a pressure (or density) lower than that in the quasiparticle calculation. In the interval between these densities, LDA predicts the existence of a Fermi surface which is consistent with the final quasiparticle result.

For xenon, the pseudopotential approximation for the electron-ion interaction is also used.[10] This approximation replaces V_n and the potential from the core electrons with a nonlocal ionic pseudopotential which eliminates the core eigenstates and the nodal structure of the valence wave functions in the core region. The vector part of the pseudopotential is retained for computing the spin-orbit interaction,[11] which is important for Xe. For hydrogen, we have used the exact $1/r$ potential.

(iii) The static dielectric matrix $\epsilon(\omega=0)$ including local-field effects is obtained from first principles[12] within the random-phase approximation (RPA): $\epsilon_{\mathrm{RPA}}=1-V_C\chi_0$, where V_C is the bare Coulomb interaction and the static independent-particle polarizability χ_0 is given by

$$\chi^0_{\mathbf{G}\mathbf{G}'}(\mathbf{q})=\frac{4}{\Omega}\sum_{c,v,\mathbf{k}}\frac{\langle v,\mathbf{k}|e^{-i(\mathbf{q}+\mathbf{G})\mathbf{r}}|c,\mathbf{k}+\mathbf{q}\rangle\langle c,\mathbf{k}+\mathbf{q}|e^{i(\mathbf{q}+\mathbf{G}')\mathbf{r}'}|v,\mathbf{k}\rangle}{\varepsilon_{v,\mathbf{k}}-\varepsilon_{c,\mathbf{k}+\mathbf{q}}} . \quad (5)$$

Here, $|i\rangle$ and ε_i are LDA eigenvectors and eigenvalues, and c and v denote the conduction and valence states, respectively. $\epsilon(\omega=0)$ is extended to finite frequencies through a generalized plasmon-pole model.[7]

These approximations result in an accuracy of the order of 0.1 eV on the band gaps of most semiconductors and insulators.[7] The method is thus expected to be of predictive power for calculations of band-gap closure under pressure.

B. Optical properties

For comparisons with experimental optical data, we have also calculated the macroscopic dielectric constant ϵ_0. The theoretical approach used in this work[12,13] involves a combination of LDA calculations with many-body corrections obtained from the quasiparticle self-energy calculations. Local-field effects are taken into account through the calculation of the full dielectric matrix $\epsilon_{\mathbf{G}\mathbf{G}'}(\mathbf{q})$. The macroscopic dielectric constant

$$\epsilon_0=\lim_{\mathbf{q}\to 0}1/\epsilon^{-1}_{\mathbf{0}\mathbf{0}}(\mathbf{q}) \quad (6)$$

is obtained from the inverse of the dielectric matrix, given by[12]

$$\epsilon^{-1}=1+V_C(1-\chi_0V_C-\chi_0K_{\mathrm{xc}})^{-1}\chi_0 . \quad (7)$$

Here, V_C is the Coulomb interaction, and K_{xc} is the functional derivative of the exchange-correlation potential with respect to density. In this work, K_{xc} is calculated within the LDA. At the scissor's operator level,[12] the many-body corrections to the LDA energies are approximated by a rigid and state-independent self Δ_{GW}. This modifies Eq. (5) in the following form:

$$\chi^0_{\mathbf{G}\mathbf{G}'}(\mathbf{q})=\frac{4}{\Omega}\sum_{c,v,\mathbf{k}}\frac{\langle v,\mathbf{k}|e^{-i(\mathbf{q}+\mathbf{G})\mathbf{r}}|c,\mathbf{k}+\mathbf{q}\rangle\langle c,\mathbf{k}+\mathbf{q}|e^{i(\mathbf{q}+\mathbf{G}')\mathbf{r}'}|v,\mathbf{k}\rangle}{\varepsilon_{v,\mathbf{k}}-\varepsilon_{c,\mathbf{k}+\mathbf{q}}-\Delta_{\mathrm{GW}}} . \quad (8)$$

Δ_{GW} could be taken to be the quasiparticle correction to the LDA minimum band gap. Because the scissor's operator preserves the wave function, it can be shown that the dipole matrix elements in Eq. (8), for $\mathbf{G}=0$, or $\mathbf{G}'=0$ and $\mathbf{q}=0$, are to be obtained from perturbation theory[12] with the LDA eigenvalues and wave functions.

We should mention that the inclusion of K_{xc} in ϵ^{-1} in Eq. (7) has very little impact on the quasiparticle energies in a semiconductor. The RPA form of the response function ϵ is consistent with the GW approximation for the self-energy where the vertex function is taken to be a δ function. However, vertex corrections do affect the optical response function and they are included at an LDA level here. This has been shown[12] to be a viable approximation when combined with χ_0 from Eq. (8). In any event, our main concerns here are the trends of the optical response function as the pressure increases. The approximations made in treating the vertex corrections are not expected to be severe in this regard.

III. RESULTS FOR XENON

In this section we present our results for the metallization of solid xenon in the hcp structure. This transition has been well characterized experimentally in both its structural and its electron properties.[4,5] The experimental results are briefly reviewed in Sec. III A. Section III B is a discussion of some previous theoretical work. Our calculational details are given in Sec. III C. Sections III D and III E contain our theoretical results, the former focusing on the spin-orbit effects in the latter on the self-energy effects. The salient features observed experimentally in the optical spectra associated with the metallization transition have been explained by the present calculation.

A. Experimental status

Until recently, the observation of metallization in solid xenon was a controversial matter.[14] However, two recent independent experiments[4,5] have given to a good precision the pressure at which xenon undergoes a metal-insulator transition. They also showed that indeed metallization occurs within the hcp structure. In these two experiments, three different optical properties have been used to characterize the transition.

(i) The metallic phase is characterized by the appearance of a sharp rise in absorption in the low-energy side of the spectra. The shape of the spectra is then fitted to a Drude model which provides an estimate of the plasma frequency as a function of pressure. The extrapolation to zero of the plasma frequency gives the metallization pressure.

(ii) In the insulating phase, the absorption spectra have an energy threshold below which there is no absorption due to the existence of the gap. Assuming an indirect band gap, the measured spectra are extrapolated to obtain an estimate of the band gap as a function of pressure. The extrapolation of the band gap to zero also gives the metallization pressure.

(iii) The appearance of a peak at ~ 2 eV in the absorption spectra has been interpreted as electronic transitions to hole states at the top of the valence band which are only available after the bands overlap. The integrated intensity of such a peak is associated with the number of free holes. The extrapolation of this intensity to zero is yet another way to determine the metallization pressure.

The simultaneous observation of all of the above is very convincing that indeed metallization has occurred and that it occurs by the band-overlap mechanism. Experimentally, procedures (i)–(iii) have all been used to determine the metallization pressure. The result is a metallization pressure of 132($\pm$5) GPa according to Ref. 4. In Ref. 5 the authors estimate the metallization to be around 150 GPa without giving an explicit estimate of the possible error bar.

The crystal structure of solid xenon has been determined by x-ray diffraction in the pressure range where metallization occurs.[5,15] For pressures above 75 GPa up to at least 172 GPa, xenon remains in the hcp structure at room temperature. Therefore, the metal-insulator transition is isostructural.

B. Previous calculations

Several previous calculations have been done with the LDA for the band-gap closure of solid xenon. Most of them[16] were carried out assuming a face-centered-cubic (fcc) structure because it was not known at the time that the relevant structure is hcp.[5,15] A recent LDA calculation has been reported for hcp xenon in the neighborhood of the metal-insulator transition.[5] However, this calculation, as well as all the previous ones, has two severe drawbacks. The first is the failure to include the many-body correction to the LDA band gap. The LDA Kohn-Sham eigenvalues are well known to underestimate the band gaps in semiconductors by up to 50% or more. The second is the neglect of spin-orbit interaction which affects the valence-band maximum complex most significantly. Xe is rather heavy, and the relativistic effects are large. As we shall show below, inclusion of both of these effects is essential for a quantitative description of the band-gap closure in solid Xe.

C. Calculation details

The Xe calculation was carried our at eight densities ranging from 0.093 to 0.077 mol/cm^3. For lower densities the hcp structure is unstable.[5,15] To compute the pressure, we use the equations of state from Refs. 4 and 5, obtained from fits to the experimental results of Refs. 15 and 5. The equation of state obtained from our LDA calculation agrees well with experiment other than a slight overestimate of 0.3% for the lattice constant. The wave functions are expanded in a plane-wave basis set with an energy cutoff of 30 Ry. We use a uniform grid of 12 $\mathbf{k}$ points in the irreducible wedge of the Brillouin zone to evaluate the charge density and potential. The dielectric matrix was evaluated on the same grid with a reciprocal-space cutoff of 3.7 a.u. We have included 390 bands for the sum over the intermediate states in Eq. (5).

D. Present results: Effects of spin-orbit interaction

Figure 1 shows the LDA band structure at the density of 0.0887 mol/cm^3 calculated *without* spin-orbit interaction. The band gap is indirect, with the valence-band maximum (VBM) at Γ and the conduction-band minimum (CBM) at K. Also notable is the twofold degeneracy at Γ at about 2 eV below the VBM. This feature has been previously considered to be responsible for[5] the observed absorption peak at 2 eV in the metallic phase mentioned in Sec. III A. But the inclusion of spin-orbit interaction changes the VBM complex drastically, and we show that the twofold degenerate states here are not relevant to the experimental observation. As the density increases, the energy of the VBM, consisting basically of antibonding $5p$ states, goes up faster than that of the CBM, which has a $5d$ bonding character. Consequently, the band gap decreases as the density increases. The non-spin-orbit LDA calculation predicts a metallization density of 0.0912 mol/cm^3, which, from the equations of state of Refs. 4 and 5, corresponds to a pressure of 123 GPa. This seems to agree rather well with experiment, but, as we shall show below, the agreement is fortuitous and is due to the accidental cancellation of two large errors.

In Fig. 2 we show the LDA band structure at the same density as that of Fig. 1, but *with* spin-orbit interaction included. The most significant effects of the spin-orbit interaction are on the splitting of the valence states at Γ close to VBM. This has three consequences.

(i) A reduction in the number of valence bands close to the VBM. This causes a reduction of about 30% in the integrated density of states in the range from the VBM down to 1.5 eV below. This low density of states might be responsible for the observed transparency of the sample even at pressures above metallization.[4,5] (The direct gap remains well above the visible range at metallization.)

(ii) A drastic change for states at Γ around 2 and 3 eV below the VBM. Interestingly, we find that there are still states at 1.9 eV. These states are most likely to be the initial states of the observed optical absorption at 2 eV. Figure 2 further suggests that spin-orbit splitting gives rise to another absorption peak at $\sim$3 eV, in addition to the 2-eV absorption that has been observed. This theoretical prediction has yet to be confirmed by experiment.

(iii) A reduction of the LDA band gap by 0.65 eV at this density. This is a considerable change and has important consequences for the predicted metallization pressure within the LDA. With spin-orbit interaction included, the LDA metallization density is at 0.0867 mol/cm^3 and the metallization pressure at 104 GPa, a 18% reduction relative to the non-spin-orbit calculation. Not surprisingly, the LDA underestimates the metallization pressure due to its underestimation of the band gap.

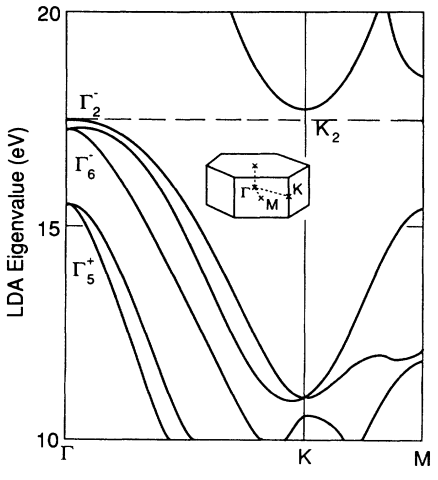

FIG. 1. LDA band structure without spin-orbit interaction for hcp xenon at the density of 0.0877 mol/cm^2. The top of the valence band is indicated by the dashed line.

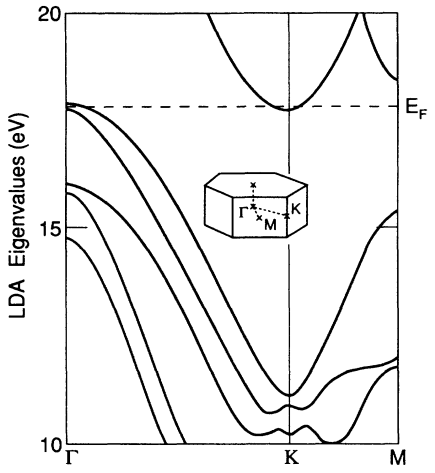

FIG. 2. The same as Fig. 1 after the inclusion of spin-orbit interaction. The Fermi level is indicated by the dashed line.

E. Quasiparticle results: effects of many-body interaction

The quasiparticle corrections calculated within the GW approximation to the LDA minimum band gap are shown in Fig. 3 in the form of $E_g(\mathrm{GW})-E_g(\mathrm{LDA})$, where $E_g(\mathrm{GW})$ and $E_g(\mathrm{LDA})$ are the quasiparticle and the LDA minimum (indirect) band gaps, respectively. Figure 3 shows two important features: First, the many-body correction decreases significantly as the density increases. This is due to an increase in the dielectric screening with density. We shall discuss this effect in more detail in Sec. IV D, in the context of our work on solid hydrogen. Second, the many-body correction is about 0.8 eV at the calculated metallization density. This large correction places the metallization density at 0.0924 mol/cm^3 and the metallization pressure at 128 GPa, in very good agreement with the experimental value[4] of 132($\pm$5) GPa.

In Fig. 4 we show the LDA and quasiparticle band gap as a function of density. In this figure we also show the experimental estimates for the band gap deduced from the absorption threshold[4] at several densities. The figure

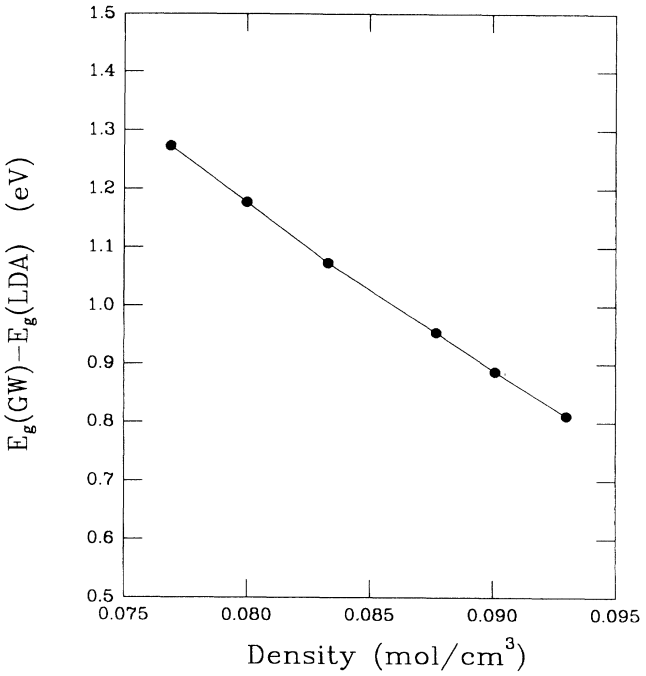

FIG. 3. Quasiparticle correction to the LDA band gap of hcp xenon as a function of density.

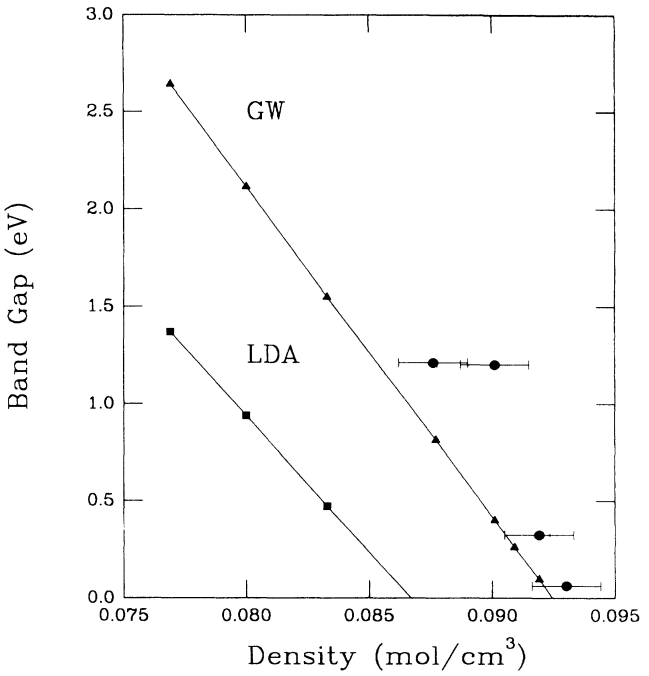

FIG. 4. LDA and quasiparticle (GW) minimum band gaps of hcp xenon as a function of density. Lines are drawn to guide the eye. The experimental results of Ref. 4 for the optical absorption threshold are also shown as solid circles.

demonstrates clearly that the GW results are in much better agreement with the experimental. In Table I, we list our results for the metallization density and pressure, together with the experimental values. Neglecting spin-orbit interaction accidentally places the LDA metallization pressure close to the experimental value. We shall discuss in more detail the trends of the many-body correction in the context of solid hydrogen under megabar pressure, where we encounter even larger changes in crystal volume.

IV. RESULTS FOR MOLECULAR SOLID HYDROGEN

The structural characterization of molecular solid hydrogen in the megabar pressure range is not nearly as certain as it is for xenon. Nor is the observation of metallization. The difficulties owe their origin to the extremely light mass of hydrogen and are encountered by experimentalists and theorists alike. Experimentally, the lightness of hydrogen makes it very difficult to perform x-ray-diffraction measurements, which are a reliable way of determining the crystal structure. The extremely high pressure and correspondingly small sample volume also make it extremely difficult to try to detect the metallization electronically. On the theoretical side, the large zero-point motion of the hydrogen molecules makes accurate total-energy calculations difficult. A perhaps more severe hindrance is that, in the insulating molecular phase, we are faced with the problem that, on the one hand, the total energy is not very sensitive to the libration of the hydrogen molecules, but, on the other hand, the

TABLE I. Experimental and theoretical results for the pressure and density at which hcp xenon undergoes metallization. Some values, indicated by an asterisk, were converted from pressure to volume or vice versa using the experimental equation of state from Refs. 4 and 5, as described in the text.

	Transition pressure (GPa)	Transition volume (cm^3/mol)
Experiment	132(5)[a]	0.0933(14)*[a]
	150[b]	0.0963*[b]
LDA, no spin-orbit	123*	0.0912
LDA	104*	0.0867
Quasiparticle	128*	0.0924

[a]Reference 4.
[b]Reference 5.

minimum band gap is very sensitive to it. The energy scales of the electronic, the vibrational, and the librational movements of a molecular hydrogen are on the order of $1:\sqrt{m_e/m_p}:m_e/m_p$. (Here, m_e and m_p are, respectively, the mass of an electron and a proton.) Crystal-field splitting will not change the order of magnitude of these energies. Complete structural characterization requires handling all these different energies accurately. This is important because the resultant quasiparticle gap depends on the structural details. We will illustrate this point using a virtual-crystal approximation.

The calculations that we report below explore the relation between atomic and electronic structures. These are accurate first-principles calculations. If the structural parameters that we used were a good correspondence to those under the experimental circumstances, our results then would provide a reliable estimate for the possible metallization. Our investigation of the effects of molecular orientational disorder at the virtual-crystal-approximation level is suggestive of what might happen when the molecules have a different orientational ordering, or no ordering at all.

In Sec. IV A we again give a brief overview of the present experimental status for the metallization of molecular solid hydrogen under pressure. Some of the previous theoretical efforts are discussed in Sec. IV B. In Sec. IV C the technical details of our calculation are given. In the balance of the Section, we report results on the variation of the band gap with density (Sec. IV D), on the effects of orientational disorder (Sec. IV E), and on the optical properties (Sec. IV F).

A. Experimental status

At low pressures, solid hydrogen is an insulator with a wide band gap, determined to be 14.5 ± 1 eV (Refs. 17 and 18) experimentally. Diamond anvil cell experiments are now able to place hydrogen samples under pressures up to 230 GPa,[19] which are high enough to reduce the molar volume by more than tenfold[20,21] relative to that at ambient pressure. Even with such a drastic compression, there has so far been no definitive evidence of hydrogen metallization. A recent debate on this subject was kindled by an observation of darkening of hydrogen samples above 200 GPa.[22] Further measurements indicated an increase in the low-frequency reflectivity of hydrogen samples at pressures above 150 GPa; this was interpreted as a fingerprint for the band-gap closure.[23] Such an interpretation has been challenged by subsequent work. Eggert *et al.*[19] claim that the absorption spectra are incompatible with metallization unless the metallic phase has an extremely low carrier density. Ruoff and Vanderborgh suggest[24] that the observed increase in reflectivity is due to the continuation of the sample by metallic aluminum above 150 GPa, caused by the reaction of ruby with hydrogen under megabar pressures. It has also been suggested[25] that vibrational transitions might be the origin of the low-energy reflectivity and absorption above 150 GPa. Therefore, unlike the case of Xe, results on the molecular-solid-hydrogen metallization from various measurements are inconclusive, and the experimental data are often interpreted in very different ways.

An alternative way to detect the onset of the insulator-metal transition is to monitor the change with pressure of the dielectric constant and its frequency derivative,[26–28] although this scheme is limited in that it only gives information on the closure of the gap for direct transitions. Several experiments have been reported[26–30] on the dielectric properties of hydrogen and deuterium under pressure. The measured quantity is the index of refraction, which can be obtained from either (a) the angular dependence of frequency shifts in Brillouin scattering[29] or (b) the angular or energy dependence of interference patterns.[30] Method (a) gives an experimental resolution of about 4% in ϵ_0 at 20 GPa (Ref. 29) versus a resolution of about 25% for method (b) at the same pressure.[30] The experimental results show that ϵ_0 increases from 1.3 to about 5 in the 0-to-73-GPa interval.[26] The behavior of ϵ_0 and its frequency derivative with pressure has been used to estimate the metallization pressure of solid H_2.[26,28] Typically, a single oscillator model for the refraction index,

$$n^2(\omega)=1+F(\omega_1^2-\omega^2) ,$$

is assumed. The derivative of $n(\omega)$ with ω is then used to compute the behavior of ω_1 with pressure, and extrapolations are used to estimate the critical pressure that corresponds to the closure of some averaged direct gap. The critical pressure thus derived varies between 150 and 400 GPa.[26,28]

As mentioned earlier, a particular difficulty associated with solid hydrogen is the limited direct experimental information on its structural properties. X-ray-diffraction measurements have only been done for pressures up to 26 GPa,[26] and up to this pressure the hcp structure is stable at 300 K.[21] Above 26 GPa, only Raman-scattering experiments have been able to give clues on the possibility of structural transformations from changes in the vibrational and rotational spectra. The disappearing of the roton bands of parahydrogen above 100 GPa at 8 K has been identified as an orientational ordering transition.[31] This interpretation, however, has been questioned.[32] For temperatures between 77 and 295 K, the roton bands persist up to at least 160 GPa, with no sign of any observable orientational transition.[32,33] Another possible sign of a structural transition has been the discovery of a discontinuity in the intramolecular vibron frequency as a function of pressure at pressures close to 150 GPa.[34,35] This discontinuity has been used as an order parameter to map out a phase diagram, in which a transition to a high-pressure phase with a critical point at 170 GPa and 150 K (Refs. 36 and 37) is identified. The nature of this phase transformation is unknown, but it has been speculated[36,37] that it corresponds to a metal-insulator transition.

B. Previous calculations

Several LDA calculations have been performed for the structural and the electronic properties of solid hydrogen under pressure.[38,39] Some of them, however, have assumed cubic structures[39,40–43] whereas current experi-

mental information[21,33] indicates that the relevant structure is hcp. A recent LDA calculation[44] has compared the enthalpies of several structures, within the Born-Oppenheimer approximation, and concluded that for pressures between 80 and 380 GPa, the hcp structure with the molecules oriented along the c axis is stable against several cubic structures and the simple hexagonal structure. Another recent LDA study,[45] also within the Born-Oppenheimer approximation, reported that a structure with the molecules on hcp sites but oriented along lower symmetry directions is marginally more stable than the structure with the molecules along the c axis.

A severe hindrance to more conclusive theoretical determination of the most stable structure, however, is the large zero-point motion energy of the hydrogen molecules,[46] which can be essential in determining the structural properties. For example, the differences in electronic energies among the different molecular orientations that we mentioned at the end of the last paragraph are smaller than the zero-point motion energy by an order of magnitude. The zero-point-motion effect can be taken into account in quantum Monte Carlo calculations,[47] but the large computational cost of this approach prevents a thorough investigation in a large structural parameter space. The influence of the rotational motion of the H_2 molecules on the band gap has also been investigated;[6,39,48] it has been predicted that the inclusion of rotational disorder increases the band gap relative to an orientationally ordered state.

C. Present calculational details

In the present study we assume an hcp structure with the H_2 molecules oriented along the c axis. Orientational disorder is considered later in Sec. IV E within a virtual-crystal approximation. The intramolecular separation is fixed at 1.40 a.u., based on results from LDA total-energy calculations.[43] Also, based on LDA calculations[43] and extrapolations of x-ray data, we use the following values for the c/a ratio: 1.580 for density ρ larger than 0.27 mol/cm^3, 1.590 for $\rho=0.23$ mol/cm^3, 1.610 for $\rho=0.195$ mol/cm^3, 1.624 for $\rho=0.167$ mol/cm^3, 1.630 for $\rho=0.125$ mol/cm^3, and 1.633 for ρ smaller than 0.1 mol/cm^3. The conversion between density and pressure in our calculation was made through the equations of state (EOS) of Refs. 20 and 21 obtained from extrapolations of experimental results at lower pressures. The difference between the two extrapolations is taken to be the uncertainties in the EOS.

The c/a ratio, the energy cutoffs used in the plane-wave expansion of the wave functions, and the reciprocal-space cutoffs used to truncate the dielectric matrix are given in Table II. In Table III we list the number of k points in the irreducible wedge of the Brillouin zone used in the summation over $\mathbf{k}$ in Eq. (8) for the calculation of the macroscopic dielectric constant.

TABLE II. Computational details for molecular solid hydrogen. E_{max} is the energy cutoff (in Ry) of the plane-wave expansion of the LDA wave function, and G_{max} (in a.u.) is the reciprocal-space cutoff of the dielectric matrix.

ρ (mol/cm^3)	c/a	E_{max}	G_{max}
0.4873	1.58	55	5.9
0.3962	1.58	55	5.5
0.3265	1.58	45	5.5
0.2723	1.58	45	5.5
0.2293	1.59	45	5.5
0.1950	1.61	45	5.5
0.1672	1.624	45	4.68
0.0967	1.633	30	4.68
0.0431	1.633	30	3.5

TABLE III. Number of points in the irreducible wedge of the Brillouin zone used in the summation over $\mathbf{k}$ in Eq. (8) for the calculation of the macroscopic dielectric constant in molecular solid hydrogen. Different grids are used for the orientationally ordered and disordered structures.

ρ (mol/cm^3)	Ordered	Disordered
0.3962		80
0.3265	252	80
0.2723	120	36
0.2293	80	36
0.1950	64	36
0.1672	36	36
0.0967	36	36
0.0431	12	12

D. Behavior of the band gap with density

In Fig. 5 we show the quasiparticle band structure for molecular solid hydrogen in the c-axis-oriented hcp structure at the density of 0.396 mol/cm^2, which is very close to the theoretical metallization density for this structure. The bands are plotted along a line from the Γ point to the K point, as shown in the inset of the figure. Both the valence-band maximum and the conduction-band

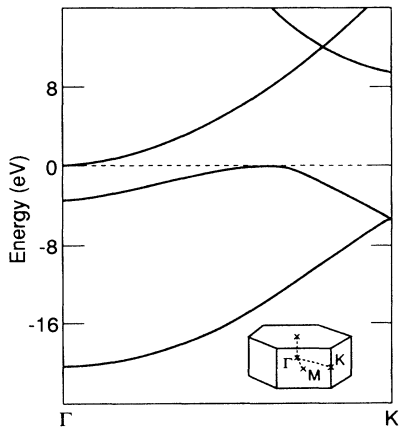

FIG. 5. Quasiparticle energy bands for molecular solid hydrogen in the orientationally ordered hcp structure at the density of 0.396 mol/cm^3. The Fermi-level (dashed line) is the origin of the energy scale.

minimum are in this direction. At this density the band gap is indirect, with the CBM at Γ and the VBM at $\sim\frac{3}{5}$ of the way from Γ to K.

The quasiparticle results for the band gaps for the c-axis-oriented hcp structure as a function of density are shown in Fig. 6. In the same figure we also show our LDA results, as well as our results from a Hartree-Fock calculation in which the HF wave functions are approximated by the LDA counterparts. A very interesting feature of Fig. 6 is the constant density derivative $dE_g/d\rho$ of the LDA and HF band gaps (the curves are almost perfect straight lines), while it is not the case for the GW results. We see from Fig. 6 that the GW results for the gap are closer to the HF results when the gaps are large, and become closer to the LDA Kohn-Sham gaps as the density increases. This qualitative feature of the GW results is not surprising since, as the density increases, the system transforms from being more atomiclike to more uniform-electron-liquid-like: in the large-gap atomic, HF is a better description than the LDA; as density increases, LDA will eventually become more appropriate.

The GW correction to the LDA band gap can be written as the sum of the correction to the VBM energy and the correction to the CBM energy. This is shown in Fig. 7, where these quantities are plotted as a function of density. The LDA potential used here is the Ceperley-Alder form. Figure 7 shows that the use of empirical corrections to LDA calculations (for instance, see Ref. 13) for the pressure dependence of the band gap would be of limited accuracy due to the large variation of the many-body corrections to the LDA band gap. This is not surprising in view of the complexities of the electron self-energy operator in real materials.[7]

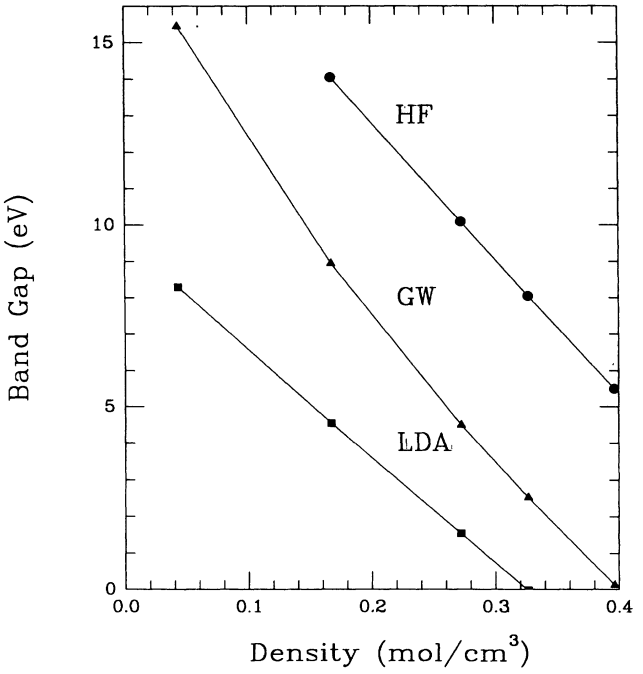

FIG. 6. Theoretical results for the minimum band gap of orientationally ordered molecular solid hydrogen in hcp structure as a function of density. Results are from quasiparticle (GW), Hartree-Fock (HF), and local-density (LDA) calculations. Lines are drawn to guide the eye.

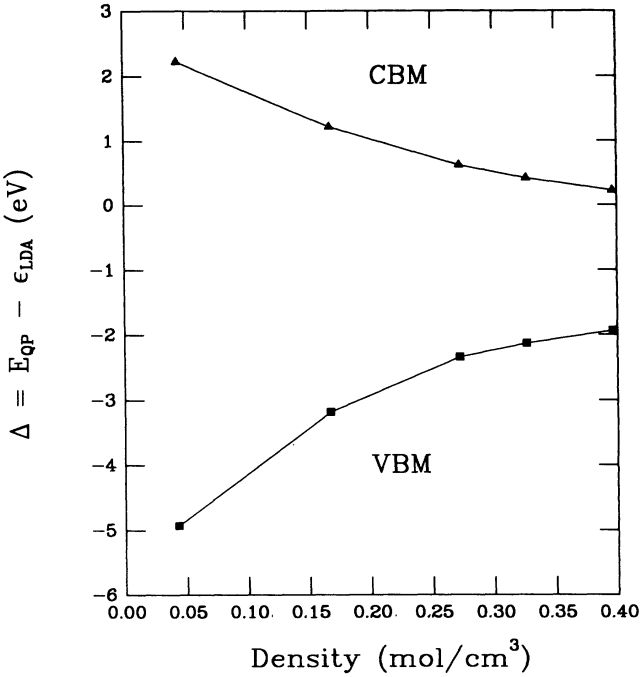

FIG. 7. Many-body correction to the LDA eigenvalues at the conduction-band minimmum (CBM) and valence-band maximum (VBM) as a function of density for orientationally ordered hcp hydrogen. Lines are drawn to guide the eye.

E. Effects of orientational disorder

An interesting property of solid H_2 is the quantum nature of the rotational degrees of freedom of the molecules, which seem to remain active up to very high pressures.[33] The large zero-point rotational (or librational) motion of the molecules is expected to have a strong effect on the optical and electric properties.[6,39,48] We have included this effect in our calculations through a virtual-crystal model. Within this model, the electrons are subjected to a proton potential averaged over an orientational distribution of the molecules. We employ a model for this distribution which is a constant for axial angles smaller than a given θ_0 and zero otherwise. The results for the electronic structure are expressed as a function of θ_0. For $\theta_0=0$ we go back to the c-axis orientationally ordered structure discussed in Sec. IV D. For $\theta_0=90°$ we have a totally orientationally disordered structure with a spherical-shell nuclear-charge distribution.[45] At any θ_0, the rotational symmetry about the c axis is retained in this model.

In Fig. 8 we show the quasiparticle band structure for $\theta_0=90°$ at a density of 0.396 mol/cm^3. By comparing with the results for $\theta_0=0$ (Fig. 5) at the same density, we see that the overall topology of the band structure is not

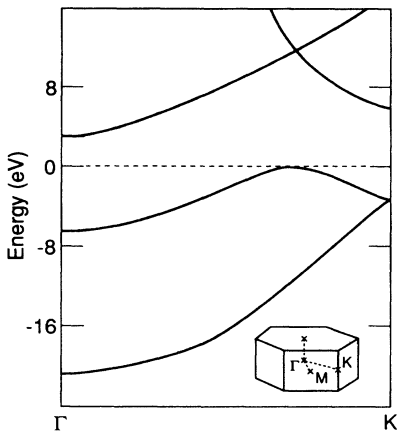

FIG. 8. The same as Fig. 5, but for the orientationally disordered hcp phase in the virtual-crystal approximation. See text for discussion.

affected by the orientational disorder with our model: the conduction-band minimum is still at Γ and the valence-band maximum is between Γ and K. The band gap, however, increases significantly with disorder. The effect of disorder on the band gap also increases with density. This can be seen in Fig. 9, where we show the quasiparticle band gaps for both orientationally ordered and disordered structure as a function of density. At low pressures, the effect of disorder on E_g is negligible, but it becomes larger as the density increases. We also show in Fig. 9 the experimental band gap at zero pressure[17,18] for solid H_2 and an experimental estimate for the band gap at 0.133 mol/cm^3 from shock-wave measurements.[49] In both cases the theoretical results lie within the experimental error bars.

The behavior of the band gap as a function of both density and orientational disorder can be understood within a tight-binding description. We decompose the wave function of the relevant states in terms of the orbitals σ_g (occupied state, even parity) and σ_u (first excited state, odd parity) and σ_u (first excited state, odd parity) of an isolated H_2 molecule. In the solid, the valence-band maximum is essentially an antibonding combination of σ_g's of the two hydrogen molecules in one hcp cell, and the conduction-band minimum is basically a bonding combination of σ_u's. The increasing overlap between molecular orbitals with increasing pressure causes an increase in the energy of the VBM states relative to the CBM states and therefore a reduction of the band gap. Further, the inclusion of orientational disorder has a stronger effect on the linear combinations of the σ_u orbitals (conduction band) due to their odd parity. As a result, the conduction-band width decreases and the band gap increases with disorder. The direct gap at Γ increases, while the direct gap at K decreases. This results in a shift of the VBM toward the K point. However, the overall bandwidths are determined by the electronic energy scale and are not much affected by these modifications to states near the gap.

We have also calculated the band-gap closure density for different values of the disorder parameter θ_0. From those calculations and from the equations of state of

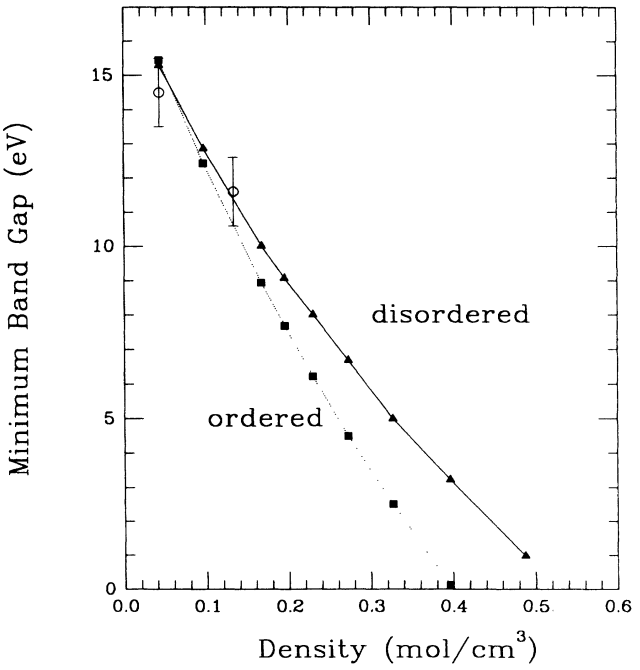

FIG. 9. Variation of the calculated minimum band gap with density for the orientationally ordered and disordered phases of hcp hydrogen. Lines are drawn to guide the eye. The experimental result sof Refs. 17 and 18 (the upper open circle) and Ref. 49 (the lower open circle) are also shown.

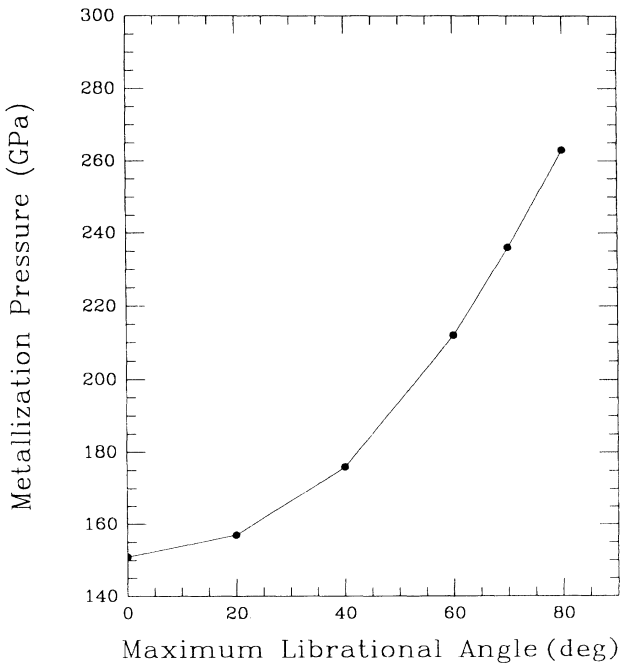

FIG. 10. Calculated metallization pressure of hcp hydrogen as a function of the maximum librational angle which characterizes the amount of orientational disorder. The line is drawn to guide the eye.

Refs. 20 and 21, we obtained theoretical metallization pressure as a function of θ_0. The results are shown in Fig. 10. The metallization pressure varies over a wide range between 150 and 300 GPa depending on the amount of disorder assumed.

F. Results for the dielectric constant

Figure 11 shows the calculated values of ϵ_0 for both orientationally ordered ($\theta_0=0$) and disordered ($\theta_0=90°$) hydrogen solids using the virtual-crystal model in the density range corresponding to pressures from zero to 240 GPa. The available experimental data for solid H_2 and D_2, extracted from measurements for the finite-frequency index of refraction, are also shown in the figure. All experimental data were converted from pressure to density through the equations of state of Refs. 20 and 21. Figure 11 shows a good agreement between theory and experiments, although there are large uncertainties in some of the experimental data at higher pressures.

Figure 11 suggests that, at high densities, the dielectric constant would undergo a catastrophe due to the closure of the direct band gap. To better understand this behavior, let us examine the average gap ω_{av} as defined in the Penn model:[50]

$$\epsilon(\omega)=1+\frac{\omega_p^2}{\omega_{av}^2-\omega^2}\ , \tag{9}$$

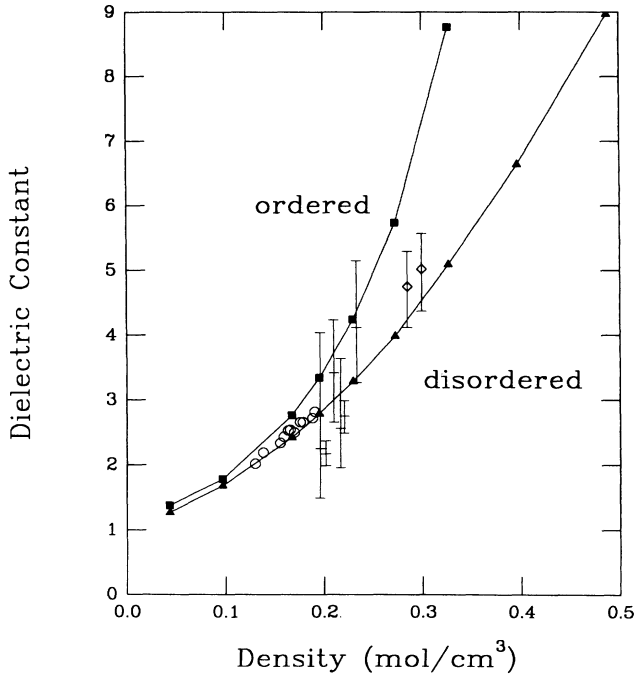

FIG. 11. Theoretical results for the static dielectric constant of hcp hydrogen for the orientationally ordered structure (squares) and for the totally orientationally disordered structure (triangles). Also shown are the experimentall results for the square of the refraction index from Ref. 29 (○), Ref. 30 (+), and Ref. 26 (◇).

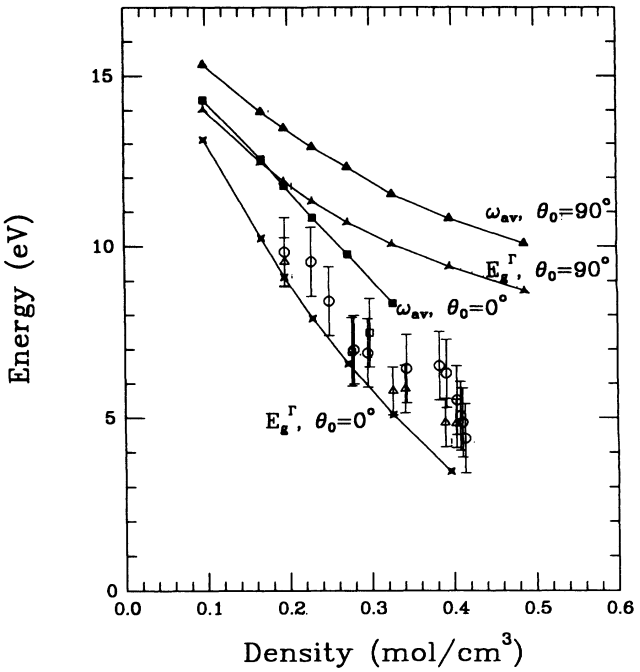

FIG. 12. Calculated direct band gap at Γ (E_g^Γ) and the average band gap (ω_{av}, obtained from the calculated dielectric constant; see text) for hcp hydrogen as a function of density. The results are for both the orientationally ordered and the orientationally disordered phases. We also show the experimental results from Ref. 28 for the single-oscillator frequency extracted from the fitting of a single-oscillator model to the frequency dependence of the refractive index.

where ω_p is the plasma frequency. ω_{av} can then be obtained from our results for ϵ_0. This is shown in Fig. 12 together with E_g^Γ, the direct quasiparticle band gap at Γ. E_g^Γ decreases with pressure and increases with orientational disorder in the same way as the minimum band gap does. The average gap calculated from Eq. (9) has a behavior similar to that of E_g^Γ for the disordered phase. This similarity is less pronounced in the ordered phase due to a stronger **k** dependence of the direct gap. Therefore, the increase of ϵ_0 with increasing order is related to the corresponding decrease of the direct gap. We also show in Fig. 12 the experimental results from Ref. 28 for the single-oscillator frequency, extracted from the fitting of a single-oscillator model to the frequency dependence of the refractive index. Although this quantity does not correspond exactly to either E_g^Γ or ω_{av}, it shows a similar behavior with density and suggests a closure of the *direct gap* at some density above 0.5 mol/cm^3, in agreement with our calculations.

V. SUMMARY

In summary, we have studied, using a first-principles quasiparticle approach, the insulator-metal transition induced by the band-overlap mechanism in solid Xe and H_2. For the case of Xe, where the structure is well characterized, our theory explains the observed features in the experimental spectra, including the metallization

pressure. The case of molecular solid hydrogen is more elusive in that details of the structural parameters are not known and are difficult to calculate theoretically. Moreover, such details have a rather large impact on the band gap, and thus on the metallization pressure. For the hcp phase in which all the molecules are perfectly aligned along the c axis, our theory predicts a metallization pressure of 150 GPa. Effects of molecular orientational disorder are shown to be important and could increase the transition pressure by as much as a factor of two.

The calculations also show that, under such drastic changes in crystal volume as are in the megabar pressure range, the quasiparticle band gaps calculated from the GW approximation are sublinear with density. The differences between the GW quasiparticle energies and the LDA eigenvalues vary with pressure in a complicated way. For solid H_2, the self-energy corrections in general decrease as the pressure increases. This is a result of the very large change in the dielectric screening of solid H_2 as the pressure is changed over the megabar range. In addition, the corrections are state dependent.

ACKNOWLEDGMENTS

We thank A. Garcia for numerous illuminating discussions. This work was supported by NSF Grant No. DMR91-20269 and by the Director, Office of Energy Research, Office of Basic Energy Sciences, Materials Sciences Division of the U.S. Department of Energy under Contract No. DE-AC03-76SF00098. H.C. acknowledges support from Conselho Nacional de Desenvolvimento Científico e Technógico, Brazil. X.Z. thanks the Center for Advanced Materials for its Support. CRAY computer time was provided by the Office of Energy Research of the U.S. Department of Energy and by the NSF at the Pittsburgh Supercomputing Center.

*Permanent address: Departamento de Física, ICEx, UFMG, C.P. 702, 30161 Belo Horizonte, Brazil.

[1]K. F. Herzfeld, Phys. Rev. **29**, 701 (1927).

[2]For a review, see F. Siringo, R. Pucci, and N. H. March, High Press. Res. **2**, 109 (1989).

[3]M. P. Pasternak, R. S. Taylor, A. Chen, C. Meade, L. M. Falicov, A. Giesekus, R. Jeanloz, and P. Yu, Phys. Rev. Lett. **65**, 790 (1990).

[4]K. A. Goettel, J. H. Eggert, I. F. Silvera, and W. C. Moss, Phys. Rev. Lett. **62**, 665 (1989).

[5]R. Reichlin, K. E. Brister, A. K. McMahan, M. Ross, S. Martin, Y. K. Vohra, and A. L. Ruoff, Phys. Rev. Lett. **62**, 669 (1989).

[6]Some preliminary results have been given in H. Chacham and S. G. Louie, Phys. Rev. Lett. **66**, 64 (1991), and also in H. Chacham, X. Zhu, and S. G. Louie, Europhys. Lett. **14**, 65 (1991).

[7]M. S. Hybertsen and S. G. Louie, Phys. Rev. Lett. **55**, 1418 (1985); Phys. Rev. B **34**, 5390 (1986). For a recent review, see, S. G. Louie, *Theory of Electronic Excitations in Solids,* in *Electronic Materials: A New Era of Materials Sciences,* edited by J. R. Chelikowski and A. Franciosi (Springer-Verlag, New York, 1991).

[8]W. Kohn and L. J. Sham, Phys. Rev. **140**, A1133 (1965).

[9]D. M. Ceperley and B. I. Alder, Phys. Rev. Lett. **45**, 566 (1980); parametrized by J. P. Perdew and A. Zunger, Phys. Rev. B **23**, 5048 (1981).

[10]D. R. Hamann, S. Schlüter, and C. Chiang, Phys. Rev. Lett. **43**, 1494 (1979); L. Kleinman, Phys. Rev. B **21**, 2630 (1980); G. B. Bachelet and M. Schluter, *ibid.* **25**, 2103 (1982).

[11]M. S. Hybertsen and S. G. Louie, Phys. Rev. B **34**, 2920 (1986).

[12]M. S. Hybertsen and S. G. Louie, Phys. Rev. B **35**, 5585 (1987).

[13]Z. H. Levine and D. C. Allan, Phys. Rev. Lett. **63**, 1719 (1989).

[14]E. N. Yakovlev, Yu. A. Timoffeev, and B. V. Vinogradov, Pis'ma Zh. Eksp. Teor. Fiz. **29**, 400 (1979) [JETP Lett. **29**, 362 (1979)]; D. A. Nelson, Jr., and A. L. Ruoff, Phys. Rev. Lett. **42**, 383 (1979); K. Syassen, Phys. Rev. B **25**, 6548 (1982); I. Makarenko, F. Weill, J. P. Itie, and J. M. Besson, *ibid.* **26**, 7113 (1982); K. S. Chan, T. L. Huang, T. A. Crzybowsky, T. J. Whetten, and A. L. Ruoff, *ibid.* **26**, 7116 (1982); K. Asaumi, T. Mori, and Y. Kondo, Phys. Rev. Lett. **49**, 837 (1982).

[15]A. P. Jephcoat, H.-K. Mao, L. W. Finger, D. E. Cox, R. J. Hemley, and C.-S. Zha, Phys. Rev. Lett. **59**, 2670 (1987).

[16]M. Ross and A. K. McMahan, Phys. Rev. B **21**, 1658 (1980); A. K. Ray, S. B. Trickey, R. S. Weidman, and A. B. Kunz, Phys. Rev. Lett. **45**, 933 (1980); J. Hama and S. Matsui, Solid State Commun. **37**, 889 (1981); A. K. Ray, S. B. Trickey, and A. B. Kunz, *ibid.* **41**, 351 (1982).

[17]A. Gedanken, B. Raz, and J. Jortner, J. Chem. Phys. **59**, 2752 (1973).

[18]K. Inoue, H. Kanzaki, and S. Suga, Solid State Commun. **30**, 627 (1979).

[19]J. H. Eggert, F. Moshary, W. J. Eans, H. E. Lorenzana, K. A. Goettel, I. F. Silvera, and W. C. Moss, Phys. Rev. Lett. **66**, 193 (1991).

[20]J. van Straaten and I. F. Silvera, Phys. Rev. B **37**, 1989 (1988).

[21]H. K. Mao, A. P. Jephcoat, R. J. Hemley, L. W. Finger, C. S. Zha, R. M. Hazen, and D. E. Cox, Science **239**, 1131 (1988).

[22]H. K. Mao and R. J. Hemley, Science **244**, 1462 (1989).

[23]H. K. Mao, R. J. Hemley, and M. Hanfland, Phys. Rev. Lett. **65**, 484 (1990).

[24]A. L. Ruoff and C. A. Vanderborgh, Phys. Rev. Lett. **66**, 754 (1991).

[25]M. Hanfland, R. J. Hemley, and H. K. Mao, Phys. Rev. B **43**, 8767 (1991).

[26]J. H. Eggert, K. A. Goettel, and I. F. Silvera, Europhys. Lett. **11**, 775 (1990); **12**, 381 (1990).

[27]J. van Straaten and I. F. Silvera, Phys. Rev. B **37**, 6478 (1988).

[28]R. J. Hemley, M. Hanfland, and H. K. Mao, Nature **350**, 488 (1991).

[29]H. Shimizu, E. M. Brody, H. K. Mao, and P. M. Bell, Phys. Rev. Lett. **47**, 128 (1981).

[30]J. van Straaten, R. J. Wijngaarden, and I. F. Silvera, Phys. Rev. Lett. **48**, 97 (1982).

[31]H. E. Lorenzana, I. F. Silvera, and K. E. Gottel, Phys. Rev. Lett. **64**, 1939 (1990).

[32]R. J. Hemley, H. K. Mao, and M. Hanfland, in *Proceedings of the Second Archimedes Workshop on Molecular Solids under Pressure, Catania, Italy, 1990,* edited by R. Pucci (Elsevier,

New York, 1990).
[33]R. J. Hemley, H. K. Mao, and J. F. Shu, Phys. Rev. Lett. **65**, 2670 (1990).
[34]R. J. Hemley and H. K. Mao, Phys. Rev. Lett. **61**, 857 (1988).
[35]H. E. Lorenzana, I. F. Silvera, and K. E. Coettel, Phys. Rev. Lett. **63**, 2080 (1989).
[36]R. J. Hemley and H. K. Mao, Science **249**, 391 (1990).
[37]H. E. Lorenzana, I. F. Silvera, and K. E. Goettel, Phys. Rev. Lett. **65**, 1901 (1990).
[38]C. Friedli and N. W. Ashcroft, Phys. Rev. B **16**, 662 (1977).
[39]A. Garcia, T. W. Barbee, III, M. Cohen, and I. F. Silvera, Europhys. Lett. **13**, 355 (1990).
[40]S. Chakavarty, J. H. Rose, D. Wood, and N. W. Ashcroft, Phys. Rev. B **24**, 1624 (1981).
[41]B. I. Min, H. J. F. Jansen, and A. J. Freeman, Phys. Rev. B **30**, 5076 (1984).
[42]B. I. Min, T. Oguchi, H. J. F. Jansen, and A. J. Freeman, Phys. Rev. B **33**, 324 (1986).
[43]B. I. Min, H. J. F. Jansen, and A. J. Freeman, Phys. Rev. B **33**, 6388 (1986).
[44]T. W. Barbee III, A. Garcia, M. Cohen, and J. L. Martins, Phys. Rev. Lett. **62**, 1150 (1989).
[45]E. Kaxiras, J. Broughton, and R. J. Hemley, Phys. Rev. Lett. **67**, 1138 (1991).
[46]K. W. Herwig, J. L. Gavillano, M. C. Schmidt, and R. O. Simmons, Phys. Rev. B **41**, 96 (1990).
[47]D. M. Ceperley and B. J. Alder, Phys. Rev. B **36**, 2092 (1987).
[48]N. W. Ashcroft, Phys. Rev. B **41**, 10 963 (1990).
[49]W. J. Nellis (private communication).
[50]D. Penn, Phys. Rev. **128**, 2093 (1962).